

Effect of a Pressure Gradient on Thermal Radiation, Heat Source, and Chemical Reaction in an Analytical Solution of an Unstable MHD Immiscible Fluid in a Porous Medium

P.R. Sakthivel and L. Sivakami *

Abstract—We possess a variety of applications in the domains associated with non-Newtonian fluids. This study aims to gain insight into the impact of the pressure quotient on a porous material, taking into multiple variables such as heat, chemical pathways, and thermal radiation. The technique begins by first modeling the formulation of partial differential equations (PDE) and using non-dimensional variables to transform them into a dimensionless form. Subsequently, the solutions are derived mitigating the Laplace technique, incorporating both the initial conditions and the boundaries. The graphs were generated using MATLAB. The outcomes of regulating metrics such as Sherwood number, Nusselt number, and skin friction are further calibrated. Then we get the resultant stress which is the exact opposite of Casson parameter γ and is also taken into account for its substantial input. It is also recorded that when the Velocity diminishes as pressure escalates, the temperature rises with an increase in thermal radiation.

Index Terms—Heat source; Laplace transform; MHD; Pressure.

I. INTRODUCTION

THE Casson fluid has garnered significant interest from researchers due to its wide-ranging applicability in practical and industrial domains. Currently, our research primarily focuses on fluids that exhibit MHD instability. To examine the characteristics of pigment scattering in oil, Casson [1] devised Casson Fluid. Md.Anwar Hossain and Alakesh Chandra Mandal [2] published, how much do factors such as free convection and mass transfer contribute to the fluid with characteristics such as viscous, electrically induced, and incompressible one along with the accelerated porous plate, which is also infinitely vertical. Umar Khan et al. [3] in their study addressed the heat transfer that arises whenever a Casson fluid is squeezed between a pair of parallel plates. Hari R. Kataria et al. [4] scrutinized the significance of radiation together with chemical interactions on the movement of a magnetohydrodynamic (MHD) Casson mixture along a trajectory which is vertical in nature that also

fluctuates and lies within the material that has numerous vessels. Yiolanda Damianou and Georgios C. Georgiou [5] carried out a study on the Poiseuille movements of a Bingham plastic with hydrophilic characteristics that fluctuate with pressure

Mohamed Abd El-Aziz et al. [6] performed the perturbation evaluation on the slip circulation and heat dissipation of Casson fluid employing vertically impervious panels with Hall current in unpredictable boundary layers. Naveed Ahmed et al. [7] did an analysis on how much influence does the magnetic trace has on the Casson fluid when the flow is considered in-between parallel plates. S. Lakshmi Priya et al. [8] measured a variety of aspects of the transfer of heat and mass on the convective dissemination of a magnetohydrodynamic (MHD) framework consisting of an immiscible base in a level channel. The study addressed how one responds to chemical compounds with the addition of a heat source. Kashif Ali Khan et al. [9] published a study conducted on the effete of the transfer of heat along with the mass on the unpredictable motion through the boundaries with a chemically-reacting Casson plasma. Asma Khalid et al. [10] tried a case study on the circulation of blood in an impermeable environment with the inclusion of carbon nanotubes (CNTs) and thermal analysis was performed.

Joby Mackolil and Basavarajappa Mahanthesh [11] worked on the precise and mathematical interpretation of the projected motion of Casson's and nanofluids in scenarios involving heat considering mass flux. Lorenzo Fusi [12] launched a study about the movement of the standardized Casson fluid featuring pressure-dependent elastic characteristics, with a special emphasis on the lubrication of surfaces. D.V. Krishna Prasad et al. [13] observed the repercussions of double-diffusive behaviours on the transmission of a Casson fluid over the frizzy slanting panel in an environment which is draconian fluid in nature and with a porous structure. Mustafa Turkyilmazoglu et al. [14] proposed a scheme for facilitating fluid motion and heat transfer which occurs in-between a disk and a cone, regardless of whether they stay stationary or swirling.

T. Salahuddin et al. [15] tested the shifting motion of a non-Newtonian Casson-type on an elongated horizontal substrate with varying thickness. Kashif Ali Abro [16] assessed the consequences of fractal-fractional derivatives used in a fluid ferromagnetic property utilizing fractal Laplace transform. The research project dealt with the preliminary issue by applying the fractal-fractional differential function. Mubbashar Nazeer et al. [17] generated a mathematical model for describing the structure and dynamics of a multi-

Manuscript received June 27, 2024; revised April 12, 2025.

P.R.Sakthivel is a research scholar at the Department of Mathematics and Statistics, Faculty of Science and Humanities, SRM Institute of Science and Technology, Kattankulathur, Chengalpattu District, Tamil Nadu-603203, INDIA. (e-mail: sr8485@srmist.edu.in).

L. Sivakami* is an Assistant Professor at the Department of Mathematics and Statistics, Faculty of Science and Humanities, SRM Institute of Science and Technology, Kattankulathur, Chengalpattu District, Tamilnadu-603203, INDIA. (corresponding author e-mail: sivakaml@srmist.edu.in).

phase stream of a fluid that is rheological Casson in character through the basic approach. T. Sravan Kumar et al. [18] investigated the phenomenon of mixed convective-radiative movement of fluids in a conduit within which, the thermal conductivity relies on temperature. Kerehalli Vinayaka Prasad et al. [19] addressed the phenomenon of peristaltic motion in the organic fluid flow augmented with Casson nano liquid acquired within a non-uniform vertical tube, focusing on its irreversibility features. Payam Jalili et al. [20] did the investigation and published the results of a nonlinear radiative heat transfer which is affected by a magnetic trace to Casson fluid that happens to be a non-Newtonian which is in a porous container. Farwa Asmat et al. [21] conducted a scientific study in the backdrop of a magnetic domain, specifically focusing on the transient nanofluid framework that includes constraints with radiant boundaries on Stoke's second problem.

Ahmed et al. [22] expressed a study focusing on the motion of a couple-stress Casson fluid across an aperture under free convection scenarios. The study used the fractional model that relied on Fourier's and Fick's laws. In a recent research investigation, Nur Fatimah Mod Omar et al [23] implored the critical clarification of the unstable Casson Fluid plus magnetohydrodynamics (MHD) over a propelling plate. Devaki et al. [24]. presented their study which dissects a steady, two- dimensional, Casson fluid which is flown through a space that is incorporated into non-uniform suction or injection in a material containing voids. In their study, G. Shankar et al. [25] shed light on the effete that Hall current along with thermal radiation play on a stream of the Williamson nanofluid through an angled ailing but working artery, while also considering the existence of heat and mass transfer. Sradharam Swain et al. [26] conducted an equilibrium analysis of the magnetohydrodynamic (MHD) stagnancy points distribution of a Casson fluid ahead of a retracting surface in a permeable substance. The research incorporated the impacts of heat absorption or release, thermal radiation, and suction. Sunitha Rani Yedhiri et al. [27] investigated the inputs of the MHD flow of an equilibrium mixture that happens to be spinning and convective, passing through an infinitely tall vertical plate. The flow is augmented by some factors namely Hall current, thermal radiation, and radiation absorption along with joule heating. P.R.Sakthivel and L.Sivakami [28] predicted the result of the same model without the pressure medium and in this current scenario, we have extended it to other metrics also. Sahu and Deka [29] extensively investigated the role stratification played on MHD flows whenever it passes an accelerated vertical slate in various environments, demonstrating significant variations in flow behavior due to temperature and diffusion changes.

Building upon the previous research, this one will explore the effect of porosity on the pressure variance and heat source in Casson fluids. The Laplace transform will be employed to solve all governing equations, and the resulting solutions will be produced using MATLAB, limited cases have been considered to verify the consistency of the results with earlier findings.

II. FORMULATION OF THE PROBLEM

The present work draws up accurate computations for the

Casson flow of fluids within the framework of factors such as radiation, pressure, and chemical observations. Here in this current scenario, we examine the trajectory of an unstable Casson fluid as it moves past a flat plate that is undergoing acceleration. The flow is restricted to the single region where $x > 0$, where x represents the lateral coordinate measured from the surface. At time t equals zero, both the medium and the plate are in a state of stillness, with identical concentration and temperature ratios. Then the plate undergoes acceleration with a velocity $u' = At$, when t is greater than 0. In Figure 1, the concentration C' and plate temperature T' are increased to T'_w and C'_w respectively.

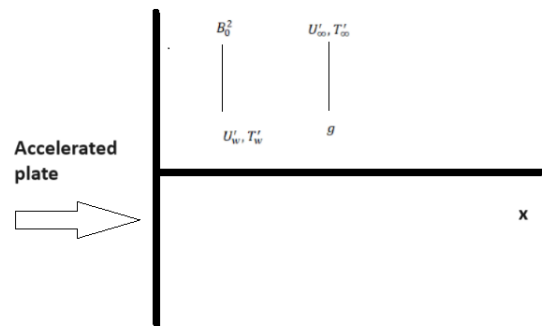


Fig. 1: Schematic flow model

II-A. Governing Equations

The movement of matter is expressed by the subsequent multifaceted expressions for momentum, energy, and concentration

$$\rho \frac{\partial u'}{\partial t'} = \mu \left(1 + \frac{1}{\gamma} \right) \frac{\partial^2 u'}{\partial x'^2} + \rho g \beta (T' - T'_{\infty}) - \sigma B_0^2 u' - \frac{\nu}{\kappa} u' + \rho g \beta^* (C' - C'_{\infty}) + \frac{\partial p}{\partial x'} \quad (1)$$

$$\rho C_p \frac{\partial T'}{\partial t'} = k \frac{\partial^2 T'}{\partial x'^2} - \frac{\partial q_r}{\partial x'} - Q_s (T' - T'_{\infty}) \quad (2)$$

$$\rho C_p \frac{\partial C'}{\partial t'} = D \frac{\partial^2 C'}{\partial x'^2} - K r' (C' - C'_{\infty}) \quad (3)$$

Within this particular framework, the symbol γ represents the Casson parameter, u' is the velocity at which the fluid crashes on the horizontal axis, t denotes a variable representing time, ν represents the kinematic viscosity, p denotes the pressure gradient, Symbols such as T' represent the fluid temperature that is nearer to the plate, β is given as the coefficient of the thermal expansion, ρ refers to the fluid density, whereas T'_{∞} denotes the temperature of the plate itself, μ refers to its dynamic viscosity, the k symbol refers to the thermal conductivity and κ refers to its porosity. q_r represents the fluid's radiative heat flux, D denotes chemical reactions occurring in the fluid, Q_s is the heat source along with starting and border conditions, whereas B is the fluid's external magnetic field, β^* is the coefficient of the concentration and the symbol C_p indicates the specific heat of the fluid represented at a constant pressure.

$$\begin{aligned} u'(x', 0) &= 0; \quad u'(0, t') = At; \quad u'(\infty, t') = 0; \\ T'(x', 0) &= T'_{\infty}; \quad T'(0, t') = T'_w; \quad T'(\infty, t') = T'_{\infty}; \\ C'(x', 0) &= C'_{\infty}; \quad C'(0, t') = C'_w; \quad C'(\infty, t') = C'_{\infty}; \end{aligned} \quad (4)$$

II-B. Non-Dimensional Analysis and Approximations

Now let us take into account the following nondimensional parameters used in the above linear equations to convert into dimensionless terminologies.

$$u = \frac{u'}{(vA)^{\frac{1}{3}}}, t = \frac{t'A^{\frac{2}{3}}}{v^{\frac{1}{3}}}, x = \frac{x'A^{\frac{1}{3}}}{v^{\frac{2}{3}}}, T = \frac{T' - T'_{\infty}}{T'_{\infty} - T'_W}, C = \frac{C' - C'_{\infty}}{C'_W - C'_{\infty}}, N = \frac{16\sigma T'_{\infty}}{3k}, M = \frac{\sigma B_0^2 v^{\frac{1}{3}}}{\rho A^{\frac{2}{3}}}, Pr = \frac{\mu C_p}{k},$$

$$Gr = \frac{g\beta(T'_W - T'_{\infty})}{A}, Gc = \frac{g\beta(C'_W - C'_{\infty})}{A}, Q = \frac{Q_s v^{\frac{1}{3}}}{\rho C_p A^{\frac{2}{3}}} \quad (5)$$

Then the Eqs. (1), (2), and (3) becomes

$$\frac{\partial u}{\partial t} = A \frac{\partial^2 u}{\partial x^2} + GrT - Bu + GcC + p \quad (6)$$

$$\lambda \frac{\partial T}{\partial t} = \frac{\partial^2 T}{\partial x^2} - QT \quad (7)$$

$$\frac{\partial C}{\partial t} = \frac{1}{Sc} \frac{\partial^2 C}{\partial x^2} - KrC \quad (8)$$

with its dimensionless initial and boundary condition:

$$u(x, 0) = 0; u(0, t) = at; u(\infty, t) = 0; \\ T(x, 0) = 0; T(0, t) = 1; T(\infty, t) = 0; \\ C(x, 0) = 0; c(0, t) = 1; C(\infty, t) = 0; \quad (9)$$

An analytical analysis is conducted to evaluate the performance of the Casson fluid which is unsteady, taking count of heat radiation and chemical reactions.

III. METHOD OF SOLUTION

The solution is derived by employing the Laplace transform scheme.

$$\frac{\partial^2 \bar{U}}{\partial x^2} + \frac{(s+B)}{A} \bar{U} = -R_1 \bar{T} - R_2 \bar{C} - R_3 \frac{1}{s} \quad (10)$$

$$\frac{\partial^2 \bar{T}}{\partial x^2} - \lambda s \bar{T} - Q \bar{T} = 0 \quad (11)$$

$$\frac{\partial^2 \bar{C}}{\partial x^2} - \bar{C}(ScKr + Scs) = 0 \quad (12)$$

The parameters utilized in this study are as follows:

$$A = 1 + \frac{1}{\gamma}, B = M + \frac{1}{k}, \lambda = \frac{Pr}{1+N}, R_1 = \frac{Gr}{A}, R_2 = \frac{Gc}{A}, R_3 = \frac{p}{A}$$

Then by applying the inverse Laplace in the equations (10),(11) and (12), we get

$$U(x, t) = U0(x, t) + U1(x, t) + U2(x, t) + U3(x, t) + U4(x, t) \quad (13)$$

Where,

$$U0(x, t) = e^{At} \left[\left(\frac{t}{2} + \frac{x}{4} \sqrt{\frac{1}{AB}} \right) \left\{ e^{x\sqrt{\frac{B}{A}}} . \operatorname{erfc} \left(\frac{x}{2\sqrt{At}} + \sqrt{Bt} \right) \right\} + \left(\frac{t}{2} - \frac{x}{4} \sqrt{\frac{1}{AB}} \right) \left\{ e^{-x\sqrt{\frac{B}{A}}} . \operatorname{erfc} \left(\frac{x}{2\sqrt{At}} - \sqrt{Bt} \right) \right\} \right] - R_3 T \quad (14)$$

$$U1(x, t) = \frac{a_1}{a_4} \left[\frac{e^{\frac{Q}{\lambda}t}}{2} \left\{ e^{-x\sqrt{Q}} . \operatorname{erfc} \left(\frac{x\sqrt{\lambda}}{2\sqrt{t}} - \sqrt{\frac{Q}{\lambda}t} \right) + e^{x\sqrt{Q}} . \operatorname{erfc} \left(\frac{x\sqrt{\lambda}}{2\sqrt{t}} + \sqrt{\frac{Q}{\lambda}t} \right) \right\} \right] - \frac{a_1}{a_4} \left[\frac{e^{\left(\frac{Q}{\lambda}+a_4\right)t}}{2} \left\{ e^{-x\sqrt{Q+a_4\lambda}} . \operatorname{erfc} \left(\frac{x\sqrt{\lambda}}{2\sqrt{t}} - \left(\sqrt{\frac{Q}{\lambda}+a_4} \right) t \right) + e^{x\sqrt{Q+a_4\lambda}} . \operatorname{erfc} \left(\frac{x\sqrt{\lambda}}{2\sqrt{t}} + \left(\sqrt{\frac{Q}{\lambda}+a_4} \right) t \right) \right\} \right] \quad (15)$$

$$U2(x, t) = \frac{a_3}{a_2} \left[\frac{e^{Krt}}{2} \left\{ e^{-x\sqrt{KrSc}} . \operatorname{erfc} \left(\frac{x\sqrt{Sc}}{2\sqrt{t}} - \sqrt{Krt} \right) + e^{x\sqrt{KrSc}} . \operatorname{erfc} \left(\frac{x\sqrt{Sc}}{2\sqrt{t}} + \sqrt{Krt} \right) \right\} \right] \quad (16)$$

$$+ e^{x\sqrt{KrSc}} . \operatorname{erfc} \left(\frac{x\sqrt{Sc}}{2\sqrt{t}} + \sqrt{Krt} \right) \left\{ e^{-x\sqrt{Sc(Kr-a_2)}} . \operatorname{erfc} \left(\frac{x\sqrt{Sc}}{2\sqrt{t}} - \sqrt{(Kr-a_2)t} \right) + e^{x\sqrt{Sc(Kr-a_2)}} . \operatorname{erfc} \left(\frac{x\sqrt{Sc}}{2\sqrt{t}} + \sqrt{(Kr-a_2)t} \right) \right\} \quad (16)$$

$$U3(x, t) = \frac{a_1}{a_4} \left[\frac{e^{(a_5-a_4)t}}{2} \left\{ e^{-x\sqrt{\frac{(a_5A_1-a_4)}{A_1}}} . \operatorname{erfc} \left(\frac{x}{2\sqrt{A_1}t} - \sqrt{(a_5-a_4)t} \right) + e^{x\sqrt{\frac{(a_5A_1-a_4)}{A_1}}} . \operatorname{erfc} \left(\frac{x}{2\sqrt{A_1}t} + \sqrt{(a_5-a_4)t} \right) \right\} \right] - \frac{a_1}{a_4} \left[\frac{e^{a_5t}}{2} \left\{ e^{-x\sqrt{\frac{a_5}{A_1}}} . \operatorname{erfc} \left(\frac{x}{2\sqrt{A_1}t} - \sqrt{a_5t} \right) + e^{x\sqrt{\frac{a_5}{A_1}}} . \operatorname{erfc} \left(\frac{x}{2\sqrt{A_1}t} + \sqrt{a_5t} \right) \right\} \right] \quad (17)$$

$$U4(x, t) = \frac{a_3}{a_2} \left[\frac{e^{B_2t}}{2} \left\{ e^{-x\sqrt{\frac{B_2}{A_2}}} . \operatorname{erfc} \left(\frac{x}{2\sqrt{A_2}t} - \sqrt{B_2t} \right) + e^{x\sqrt{\frac{B_2}{A_2}}} . \operatorname{erfc} \left(\frac{x}{2\sqrt{A_2}t} + \sqrt{B_2t} \right) \right\} \right] - \frac{a_3}{a_2} \left[\frac{e^{(B_2+a_2)t}}{2} \left\{ e^{-x\sqrt{\frac{B_2+a_2}{A_2}}} . \operatorname{erfc} \left(\frac{x}{2\sqrt{A_2}t} - \sqrt{(B_2+a_2)t} \right) + e^{x\sqrt{\frac{B_2+a_2}{A_2}}} . \operatorname{erfc} \left(\frac{x}{2\sqrt{A_2}t} + \sqrt{(B_2+a_2)t} \right) \right\} \right] \quad (18)$$

$$\text{with } a_1 = \frac{AR_1}{A\lambda-1}; -a_2 = \frac{AKrSc-B}{ASC-1}; a_3 = \frac{AR_2}{ASC-1}; -a_4 = \frac{AQ-B}{A\lambda-1}; a_5 = \frac{B+1}{A\lambda}$$

$$T(x, t) = \frac{e^{\frac{Q}{\lambda}t}}{2} \left\{ e^{-x\sqrt{\frac{Q}{\lambda}}} . \operatorname{erfc} \left(\frac{x\sqrt{\lambda}}{2\sqrt{t}} - \sqrt{\frac{Q}{\lambda}t} \right) + e^{x\sqrt{\frac{Q}{\lambda}}} . \operatorname{erfc} \left(\frac{x\sqrt{\lambda}}{2\sqrt{t}} + \sqrt{\frac{Q}{\lambda}t} \right) \right\} \quad (19)$$

$$C(x, t) = \frac{e^{krt}}{2} \left\{ e^{-x\sqrt{KrSc}} . \operatorname{erfc} \left(\frac{x\sqrt{Sc}}{2\sqrt{t}} - \sqrt{Krt} \right) + e^{x\sqrt{KrSc}} . \operatorname{erfc} \left(\frac{x\sqrt{Sc}}{2\sqrt{t}} + \sqrt{Krt} \right) \right\} \quad (20)$$

IV. SKIN FRICTION

Skin friction is denoted by τ , and it is calculated by using the equations (14) – (18) in,

$$\tau^*(x, t) = -\mu \left(1 + \frac{1}{\gamma} \right) \tau, \text{ where } \tau = \frac{\partial U}{\partial x} \Big|_{x=0} \\ \tau(x, t) = \tau_0(x, t) + \tau_1(x, t) + \tau_2(x, t) + \tau_3(x, t) + \tau_4(x, t) \quad (21)$$

Where,

$$\tau_0(x, t) = e^{At} \left[\frac{1}{4} \sqrt{\frac{1}{AB}} . \operatorname{erfc}(\sqrt{Bt}) + \frac{t}{2} . \sqrt{\frac{B}{A}} . \operatorname{erfc}(\sqrt{Bt}) + \frac{t}{2} . \operatorname{erfc}(\sqrt{Bt}) \right] \quad (22)$$

$$\tau_1(x, t) = \frac{a_1}{a_4} \left[e^{\frac{Q}{\lambda}t} . \sqrt{Q} . \operatorname{erfc} \left(\sqrt{\frac{Q}{\lambda}t} \right) - \sqrt{Q+a_4\lambda} . e^{\left(\frac{Q}{\lambda}+a_4\right)t} \operatorname{erfc} \left(\sqrt{\left(\frac{Q}{\lambda}+a_4\right)t} \right) \right] \quad (23)$$

$$\tau_2(x, t) = \frac{a_3}{a_2} \left[\sqrt{KrSc} . e^{krt} . \operatorname{erfc}(\sqrt{Krt}) - \sqrt{(Kr+a_2)Sc} . e^{(Kr+a_2)t} . \operatorname{erfc}(\sqrt{(kr+a_2)t}) \right] \quad (24)$$

$$\begin{aligned} \tau_3(x, t) &= \frac{a_1}{a_4} \left[\sqrt{\frac{(a_5 A_1 - a_4)}{A_1}} \cdot e^{(a_5 - a_4)t} \cdot \operatorname{erfc}(\sqrt{(a_5 - a_4)t}) \right. \\ &\quad \left. - \sqrt{\frac{a_5}{A_1}} \cdot e^{a_5 t} \cdot \operatorname{erfc}(\sqrt{a_5 t}) \right] \end{aligned} \quad (25)$$

$$\begin{aligned} \tau_4(x, t) &= \frac{a_3}{a_2} \left[\sqrt{\frac{B_2}{A_2}} \cdot e^{B_2 t} \cdot \operatorname{erfc}(\sqrt{B_2 t}) \right. \\ &\quad \left. - \sqrt{\frac{B_2 + a_2}{A_2}} \cdot e^{(B_2 + a_2)t} \cdot \operatorname{erfc}(\sqrt{(B_2 + a_2)t}) \right] \end{aligned} \quad (26)$$

V. NUSSELT NUMBER

Expressions of Nusselt number Nu , $Nu = - \left(\frac{\partial T}{\partial x} \right)_{x=0}$, using equation (19), we obtained the Nusselt number.

$$Nu = \frac{\sqrt{\lambda}}{\sqrt{\pi t}} - \sqrt{\frac{Q}{\lambda}} \cdot e^{\frac{Q}{\lambda} t} \cdot \operatorname{erfc} \left(\sqrt{\frac{Q}{\lambda} t} \right) \quad (27)$$

VI. SHERWOOD NUMBER

It is denoted by Sh , and the definition for Sherwood Number is, $Sh = - \left(\frac{\partial C}{\partial x} \right)_{x=0}$ using equation (20), we have gotten the result which is expressed as.

$$Sh = \frac{\sqrt{Sc}}{\sqrt{\pi t}} - \sqrt{Kr Sc} \cdot e^{krt} \cdot \operatorname{erfc}(\sqrt{krt}) \quad (28)$$

TABLE I

LOCAL SKIN FRICTION VARIATION

Comparison of Skin friction variation in the presence of $Pr = 0.71$, $t=0.4$ and $\gamma = 0.1$ and in the absence of p, Q, Kr

Skin friction variation							
Sc	Gr	Gc	κ	M	N	Hari R. Kataria et al. [4]	Current Analysis
0.6	2	5	0.4	0.5	0.5	2.7934	2.9292
0.7	2	5	0.4	0.5	0.5	2.7197	2.9030
0.8	2	5	0.4	0.5	0.5	2.6561	2.8808
0.6	3	5	0.4	0.5	0.5	3.4741	2.8813
0.6	5	5	0.4	0.5	0.5	4.8355	2.7856
0.6	2	7	0.4	0.5	0.5	3.3663	2.4490
0.6	2	9	0.4	0.5	0.5	3.9391	1.9688
0.6	2	5	0.5	0.5	0.5	2.5466	4.0269
0.6	2	5	0.4	0.7	0.5	2.9362	2.5793
0.6	2	5	0.4	0.9	0.5	3.0545	2.2700
0.6	2	5	0.4	0.9	0.7	2.0626	2.9902
0.6	2	5	0.4	0.9	0.8	1.8636	3.0242

TABLE II

LOCAL NUSSELT NUMBER

Nusselt number when $Pr = 0.71$, and in the absence of N, Q

Nusselt Number variation		
t	Hari R. Kataria et al. [4]	Current Analysis
0.4	0.2026	0.3007
0.5	0.2758	0.3362
0.6	0.3534	0.3682
0.7	0.4291	0.3977
0.8	0.5021	0.4252

TABLE III

LOCAL SHERWOOD NUMBER

Sherwood Number in the presence of t and Sc and the absence of Kr

Sherwood Number variation			
t	Sc	Hari R. Kataria et al. [4]	Current Analysis
0.4	0.6	0.2532	0.2764
0.4	0.7	0.2734	0.2985
0.4	0.8	0.2923	0.3192
0.5	0.6	0.3414	0.3090
0.6	0.6	0.4334	0.3385

VII. RESULTS AND DISCUSSION

Here, the resultant of the temperature, concentration, and velocity that is for an electrically charged, viscous fluid in the porous state are calculated by MATLAB with factors such as $Gr=1$, $Gc=1$, $Pr=20$, $p=1$, $Q=4$, $k=0.2$, $M=5$, $N=3$, $t=0.33$, $Sc=3$, $kr=1$, and $\gamma=0.2$.

Figure 2(a) demonstrates the influence of the radiation constraint over temperature. Increasing the radiation parameter gives a raise in the temperature field. Figure 2(b) illustrates about temporal variation of the temperature profile. The temperature gradually increases over time. Figure 2(c) features the heat source in respect to the coefficient of temperature. Where we can clearly see that the temperature increases when the heat source increases.

Figure 3(a) highlights that the concentration trace worsens as the chemical tolerance attribute increases. Figure 3(b) demonstrates the detrimental position of the Schmidt number in the concentration section. Observations indicate that the concentration diminishes as the Schmidt level increases.

Figure 4(a) showcases the favorable implications of Schmidt number regarding velocity. The graph shows that the velocity escalates as the Schmidt level advances. Figure 4(b) illustrates how the metrics of the Chemical reaction correspond to the velocity domain. When there is a rise in the kr number, the flow velocity increases. The porosity parameter κ is illustrated in Figure 4(c) for velocity profiles. The velocity reduces proportionally as κ lowers. In Figure 4(d) we observe that velocity diminishes as the value of M increases. This is anticipated because the Lorentz force slows down the movement in the velocity field. Figure 4(e), shows that the values concerning velocity diminish as the values of N grows. Figure 4(f) illustrates the t 's impact on the velocity curve u . As t grows, the velocity u increases. Figure 4(g) shows the impact of variable p in accordance with the velocity u . As the p grows, the velocity reduces. Figure 4(h) gives us the impact of a declining trend in the Casson parameter on the velocity. Figure 4(i), illustrates the impacts of the heat source, which when increased, the velocity increases. The relationship between heat and velocity is directly proportional, meaning that when the heat is increased, velocity also increases. Figure 4(j), depicts control of the Pr number on the velocity profile. A jump in the Prandtl quantity correlates with a spike in velocity.

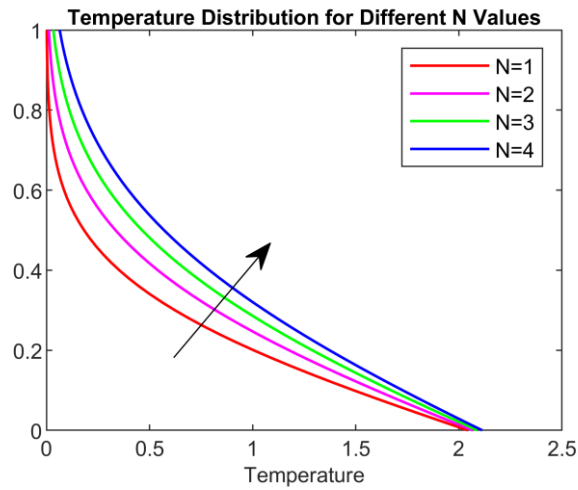


Figure 2(a) Patterns of the temperature gradient for diverse counts of N with constraints $Pr=20$, $t=0.33$, and $Q=4$

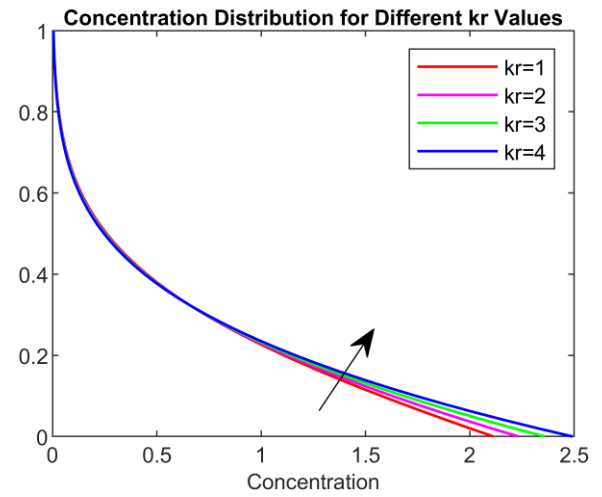


Figure 3(a) Patterns of the concentration gradient for diverse counts of Kr with constraints $Sc=3$, $t=0.33$

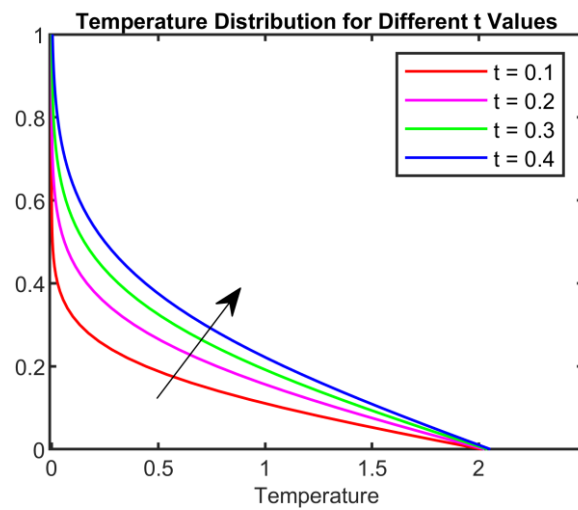


Figure 2(b) Patterns of the temperature gradient for diverse counts of time with constraints $Pr=20$, $N=3$, and $Q=4$

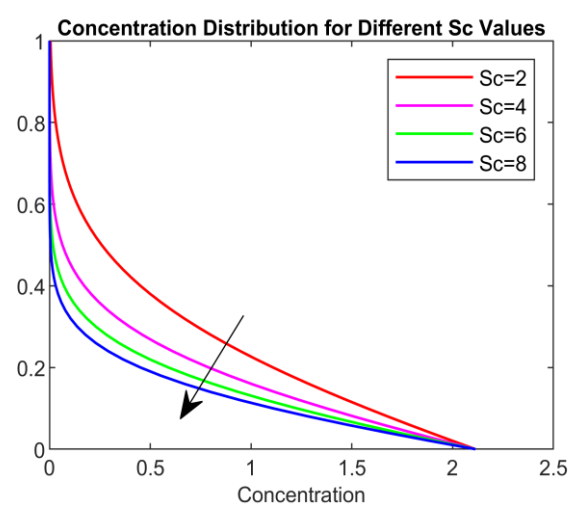


Figure 3(b) Patterns of the concentration gradient for diverse counts of the Sc with constraints $kr=1$, $t=0.33$

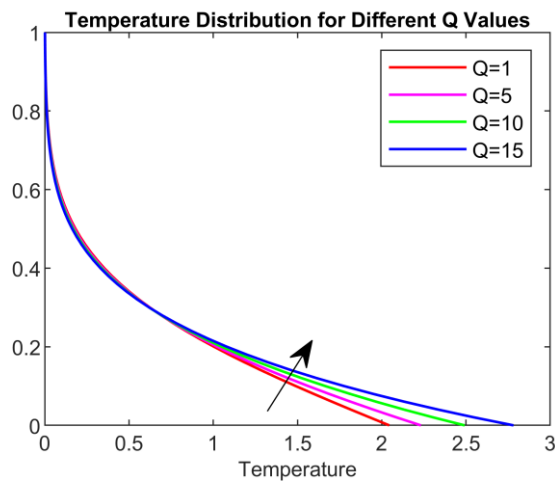


Figure 2(c) Patterns of temperature gradient for diverse counts of heat source (Q) with constraints $Pr=20$, $N=3$, and $t=0.33$

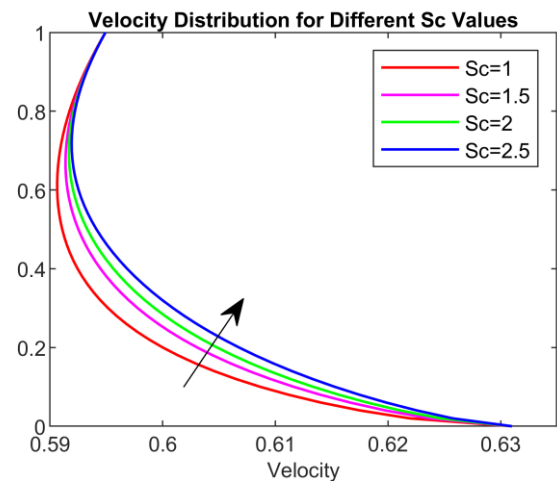


Figure 4(a) Patterns of the velocity gradient for diverse counts of the Sc with constraints $Gr=1$, $\gamma=0.2$, $p=1$, $Pr=20$, $k=0.2$, $M=5$, $N=3$, $t=0.33$, $kr=1$, $Q=4$, $Gc=1$

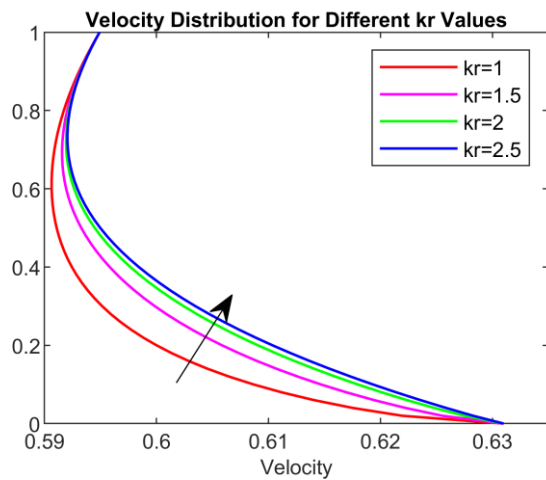


Figure 4(b) Patterns of velocity gradient for diverse counts of Kr with the constraints $Gr=1$, $\gamma=0.2$, $p=1$, $Pr=20$, $k=0.2$, $M=5$, $N=3$, $t=0.33$, $Sc=1$, $Q=4$, $Gc=1$

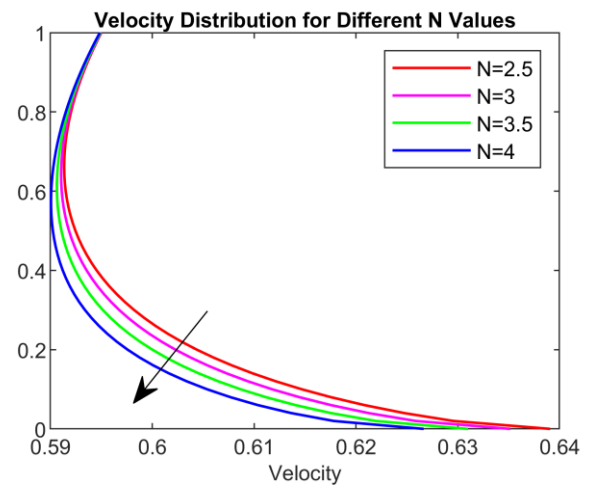


Figure 4(e) Patterns of the velocity gradient for diverse counts of the thermal quotient (N) with constraints $Gr=1$, $\gamma=0.2$, $p=1$, $Pr=20$, $k=0.2$, $M=5$, $t=0.33$, $Sc=1$, $Q=4$, $Gc=1$, $kr=1$

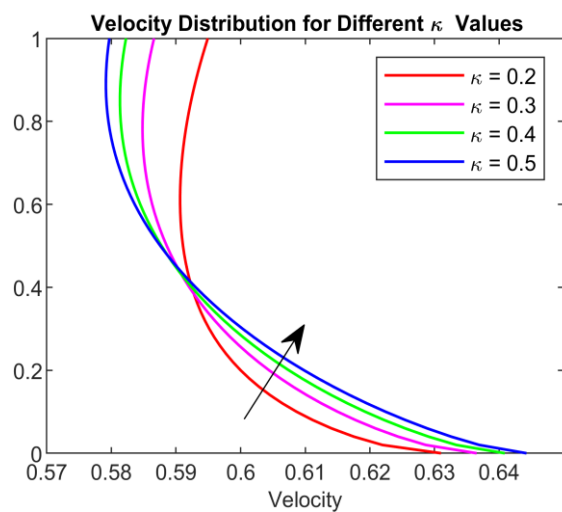


Figure 4(c) Patterns of velocity gradient for diverse counts of porosity parameter (κ) with constraints $Gr=1$, $\gamma=0.2$, $p=1$, $Pr=20$, $M=5$, $N=3$, $t=0.33$, $Sc=1$, $Q=4$, $Gc=1$, $kr=1$

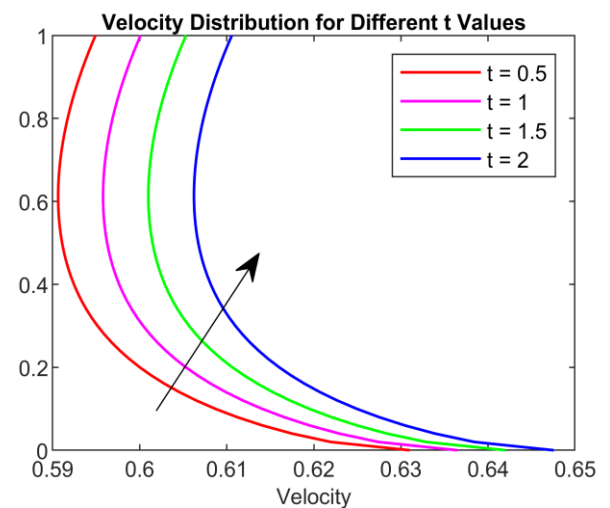


Figure 4(f) Patterns of the velocity gradient for diverse counts of the t with constraints $Gr=1$, $\gamma=0.2$, $p=1$, $Pr=20$, $k=0.2$, $M=5$, $N=3$, $kr=1$, $Sc=1$, $Q=4$, $Gc=1$

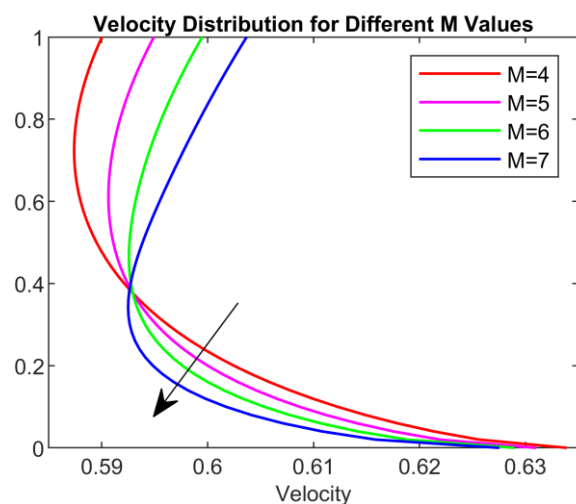


Figure 4(d) Patterns represented in the velocity gradient for diverse counts of the parameter (M) with constraints $Gr=1$, $\gamma=0.2$, $p=1$, $Pr=20$, $k=0.2$, $N=3$, $t=0.33$, $Sc=1$, $Q=4$, $Gc=1$, $kr=1$

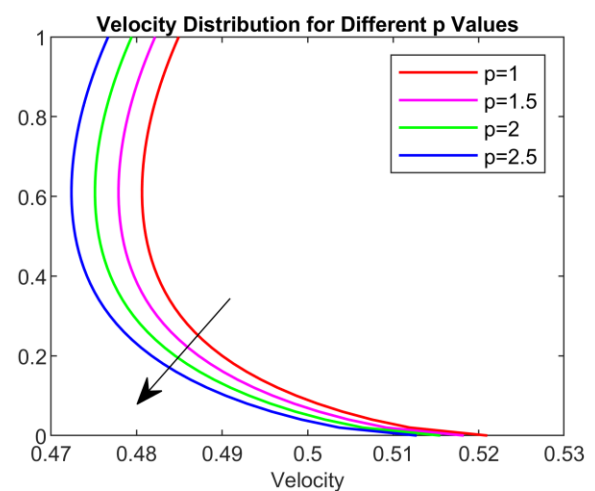


Figure 4(g) Patterns of the velocity gradient for diverse counts of the pressure (p) with constraints $Gr=1$, $\gamma=0.2$, $Pr=20$, $k=0.2$, $M=5$, $N=3$, $t=0.33$, $Sc=1$, $Q=4$, $Gc=1$, $kr=1$

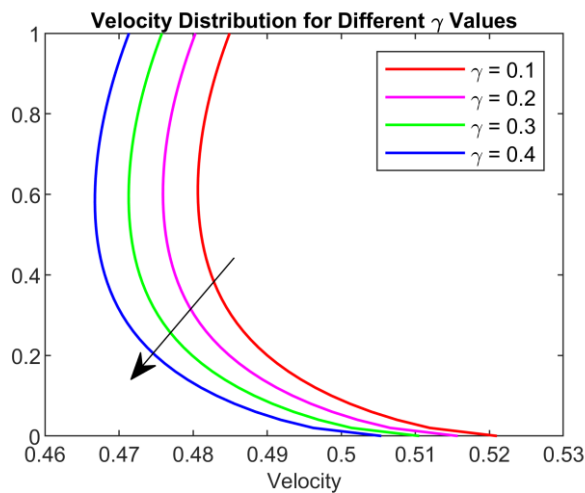


Figure 4(h) Patterns of the velocity gradient for diverse counts of the Casson parameter with constraints $Gr=1$, $kr=1$, $p=1$, $Pr=20$, $k=0.2$, $M=5$, $N=3$, $t=0.33$, $Sc=1$, $Q=4$, $Gc=1$

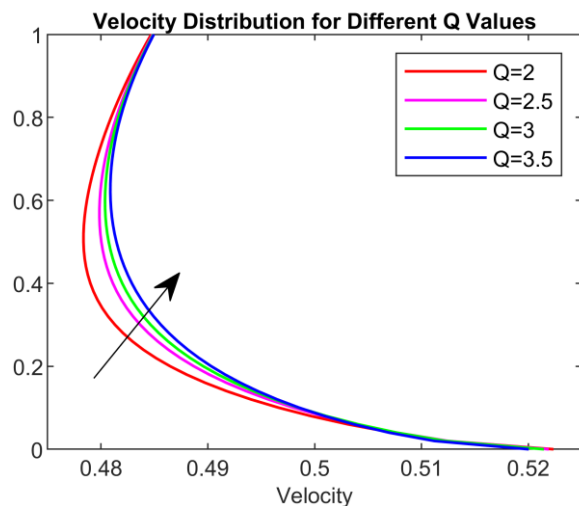


Figure 4 (i) Patterns of the velocity gradient for diverse counts of the heat source with constraints $Gr=1$, $\gamma=0.2$, $p=1$, $Pr=20$, $k=0.2$, $M=5$, $N=3$, $t=0.33$, $Sc=1$, $Gc=1$, $kr=1$

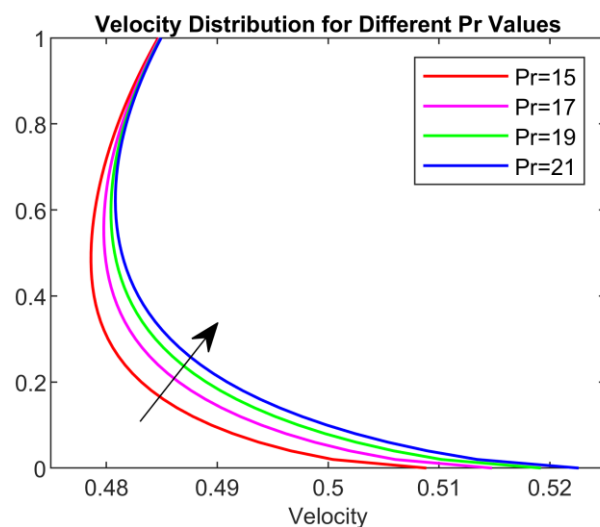


Figure 4 (j) Patterns of the velocity gradient for diverse counts of the Prandtl number constraints $Gr=1$, $\gamma=0.2$, $p=1$, $k=0.2$, $M=5$, $N=3$, $t=0.33$, $Sc=1$, $Q=4$, $Gc=1$, $kr=1$

VIII. CONCLUSION

The current analysis is conducted to determine the performance of a Casson fluid in an unsteady mode, along with metrics like chemical reactions, heat radiation, and pressure. The solution comes through the utilization of the Laplace transform technique.

- It is noted that there is a direct correlation between the increase in temperature and the spike in thermal radiation, time, and heat source.
- In addition, as we keep increasing the chemical reaction constraint, there is an increase in concentration, and when Schmidt quantity is increased, there is a drop in the fluid concentration.
- The study concludes that higher levels of magnetic parameters, thermal radiation, Pressure, and Casson parameters result in the velocity field drop.
- On the other hand, if we move up the values of the Schmidt Number, the Chemical reaction, porous media, time, Heat source, and Prandtl number, we find that the velocity also increases.
- The deviations of Nusselt Number, Sherwood Number, and Skin friction for the count when $Pr = 0.71$ are illustrated in Tables 1–3 for various combinations of the regulating metrics.
- Increases in Thermal radiation, Sc , and κ cause skin friction to rise, whereas increases in Gr , Gc , and M cause it to fall.
- On the other hand, the Nusselt number goes up whenever there is a rise in t .
- Increasing the Sc and t indicators entails an increase in the Sherwood number.
- According to the data exhibited in Tables 1 and 3, we assessed that the range of Nusselt Number along with Skin friction rises whenever there is an increase with Pr .

REFERENCES

- [1] Casson N. A flow equation for pigment-oil suspensions of the printing ink type. *Rheology of Disperse Systems*, 1959: pp84–104.
- [2] Md.Anwar Hossain and Alakesh Chandra Mandal., “Mass transfer effects on the unsteady hydromagnetic free convection flow past an accelerated vertical porous medium plate,” *Journal of Physics D: Applied Physics.*, vol. 18, no.7, 1985.
- [3] Umar Khan., Sheikh Irfanullah Khan., Naveed Ahmed Ahmed., Saima Bano and Syed Tauseef Mohyud-Din., “Heat transfer analysis for squeezing flow of a Casson fluid between parallel plates,” *Ain Shams Engineering Journal.*, vol. 7, no.1, pp497-504, 2016.
- [4] Hari R. Kataria., and Harshad R. Patel., “Radiation and chemical reaction effects on MHD Casson fluid flow past an oscillating vertical plate embedded in porous medium,” *Alexandria Engineering Journal.*, vol. 55, no.1, pp583-595, 2016.
- [5] Yiolanda Damianou., and Georgios C. Georgiou., “On Poiseuille flows of a Bingham plastic with pressure-dependent rheological parameters,” *Journal of Non-Newtonian Fluid Mechanics.*, vol. 250, pp1-7, 2017.
- [6] Mohamed Abd El-Aziz., and Aishah S. Yahya., “Perturbation analysis of unsteady boundary layer slip flow and heat transfer of Casson fluid past a vertical permeable plate with Hall current,” *Applied Mathematics and Computation.*, vol. 307, pp146-164, 2017.
- [7] Naveed Ahmed., Umar Khan., Sheikh Irfanullah Khan., Saima Bano., and Syed Tauseef Mohyud-Din., “Effects on magnetic field in squeezing flow of a Casson fluid between parallel plates,” *Journal of King Saud University–Science.*, vol. 29, no.1, pp119-125, 2017.
- [8] S.Lakshmi Priya., A. Govindarajan., L. Sivakami., “Heat and mass transfer effect on MHD convective flow of immiscible fluid in a horizontal channel in the presence of chemical reaction and heat

- source,” *International Journal of Pure and Applied Mathematics.*, vol. 113, no.13, pp252-26, 2017.
- [9] Kashif Ali Khan., Asma Rashid Butt., Nauman Raza., “Effects of heat and mass transfer on unsteady boundary layer flow of a chemical reacting Casson fluid,” *Results in Physics.*, vol. 8, pp610-620, 2018.
- [10] Asma Khalid., Ilyas Khan., Arshad Khan., Sharidan Shafie., I. Tlili., “Case study of MHD blood flow in a porous medium with CNTs and thermal analysis,” *Case Studies in Thermal Engineering.*, vol. 12, pp374-380, 2018.
- [11] Joby Mackolil., and Basavarajappa Mahanthesh., “Exact and statistical computations of radiated flow of nano and Casson fluids under heat and mass flux conditions,” *Journal of Computational Design and Engineering.*, vol. 6, no. 4, pp593-605, 2019.
- [12] Lorenzo Fusi., “Lubrication flow of a generalized Casson fluid with pressure-dependent rheological parameters,” *Journal of Non-Newtonian Fluid Mechanics.*, vol. 274, 2019.
- [13] D.V. Krishna Prasad., G.S. Krishna Chaitanya., R. Srinivasa Raju., “Double diffusive effects on mixed convection Casson fluid flow past a wavy inclined plate in presence of Darcian porous medium,” *Results in Engineering.*, vol. 3, 2019.
- [14] Mustafa Turkiymazoglu., “On the fluid flow and heat transfer between a cone and a disk both stationary or rotating,” *Mathematics and Computers in Simulation.*, vol. 177, pp329-340, 2020.
- [15] T. Salahuddin., Nazim Siddique., and Maryam Arshad., “Insight into the dynamics of the non-Newtonian Casson fluid on a horizontal object with variable thickness,” *Mathematics and Computers in Simulation.*, vol. 177, pp211-231, 2020.
- [16] Kashif Ali Abro., “Role of fractal–fractional derivative on ferromagnetic fluid via fractal Laplace transform: A first problem via fractal–fractional differential operator,” *European Journal of Mechanics-B/Fluids.*, vol. 85, pp76-81, 2021.
- [17] Mubbashar Nazeer., Farooq Hussain., M.K. Hameed., M. Ijaz Khan., Fayyaz Ahmad., M.Y. Malik., Qiu-Hong Shi., “Development of mathematical modeling of multi-phase flow of Casson rheological fluid: Theoretical approach,” *Chaos, Solitons & Fractals.*, vol. 150, 2021.
- [18] T. Sravan Kumar., D.N. Punith Kumar., and A. Sreevallabha Reddy., “Study of mixed convective–radiative fluid flow in a channel with temperature-dependent thermal conductivity,” *Partial Differential Equations in Applied Mathematics.*, vol. 5, 2022.
- [19] Kerehalli Vinayaka Prasad., Hanumesh Vaidya., Fateh Mebarek Oudina., Khalid Mustafa Ramadan., Muhammad Ijaz Khan., Rajashekhar Choudhari., Rathod Kirankumar Gulab., Iskander Tlili., Kamel Guedri., Ahmed M. Galal., “Peristaltic activity in blood flow of Casson nanoliquid with irreversibility aspects in vertical non-uniform channel,” *Journal of the Indian Chemical Society.*, vol. 99, no. 8, 2022.
- [20] Payam Jalili., Ali Ahmadi Azar., Bahram Jalili., and Davood Domiri Ganji., “Study of nonlinear radiative heat transfer with magnetic field for non-Newtonian Casson fluid flow in a porous medium,” *Results in Physics.*, vol. 48, 2023.
- [21] Farwa Asmat., W.A. Khan., Usman., Ilyas Khan., Taseer Muhammad., “A scientific report on Stokes' second problem for a transient nanofluid model with a heated boundary in the presence of a magnetic field,” *Journal of Magnetism and Magnetic Materials.*, vol. 586, 2023.
- [22] S. Ahmad., S. U. Haq., F. Ali., I. Khan and S. M. Eldin., “Free convection channel flow of couple stress Casson fluid: a fractional model using Fourier's and Fick's laws,” *Frontiers in Physics.*, vol. 11, 2023.
- [23] Nur Fatimah Mod Omar., Husna Izzati Osman., Ahmad Qushairi Mohamad., Rahimah Jusoh., Zulkhibri Ismail., “Analytical Solution of Unsteady MHD Casson Fluid with Thermal Radiation and Chemical Reaction in Porous Medium,” *Journal of Advanced Research in Applied Sciences and Engineering Technology.*, vol. 29, no.2, pp185-194, 2023.
- [24] B. Devaki., V. S. Sampath Kumar, and P Pai. Nityananda, “Analysis of Casson Flow Through Parallel and Uniformly Porous Walls of Different Permeability,” *IAENG International Journal of Applied Mathematics.*, vol. 53, no.1, pp9-16, 2023.
- [25] G. Shankar., E.P. Siva., “A Numerical Investigation of Thermal and Mass Exchange of Blood Along Porous Stenosis Arterial Flow with Applied Magnetic Field,” *IAENG International Journal of Applied Mathematics.*, vol. 54, no.3, pp532-541, 2024.
- [26] Sradharam Swain., Golam Mortuja Sarkar., and Bikash Sahoo., “Stability analysis of MHD stagnation point flow of Casson fluid past a shrinking sheet in porous medium considering heat sink or source, thermal radiation and suction effects,” *Journal of Computational Science.*, vol. 75, 2024.
- [27] Sunitha Rani Yedhiri., Kalyan Kumar Palaparthi., Raghunath Kodi., and Farwa Asmat., “Unsteady MHD rotating mixed convective flow through an infinite vertical plate subject to Joule heating, thermal radiation, Hall current, radiation absorption,” *Journal of Thermal Analysis and Calorimetry.*, 2024.
- [28] P.R.Sakthivel., and L.Sivakami., “Analytical solution of unsteady MHD immiscible fluid with thermal radiation and chemical reaction in a porous medium under heat source”, *Journal of Interdisciplinary Mathematics.*, vol 27, no 5, pp1017-1027, 2024.
- [29] D. Sahu., and R.K. Deka., “Influence of thermal stratification and chemical reaction on MHD free convective flow along an accelerated vertical plate with variable temperature and exponential mass diffusion in a porous medium,” *Heat Transfer.*, vol. 53, no. 7, pp3643-3666, 2024.